Characterization of a human–pathogenic *Acanthamoeba griffini* isolated from a contact lens-wearing keratitis patient in Spain

I. HEREDERO-BERMEJO[1], A. CRIADO-FORNELIO[1]*, I. DE FUENTES[2], J. SOLIVERI[1], J. L. COPA-PATIÑO[1] *and* J. PÉREZ-SERRANO[1]

[1] *Departamento de Biomedicina y Biotecnología, Grupo ECOMYP, Facultad de Farmacia, Universidad de Alcalá, 28871 Alcalá de Henares, Madrid, Spain*
[2] *Servicio de Parasitología, Centro Nacional de Microbiología, Instituto de Ciencias de la Salud Carlos III, Carretera Majadahonda-Pozuelo km 2, 28224 Majadahonda, Madrid, Spain*

(*Received 11 March 2014; revised 6 May and 26 June 2014; accepted 28 June 2014; first published online 28 July 2014*)

SUMMARY

Amoebae were isolated from contact lenses of a symptomatic lens wearer in Spain. Protozoa were characterized by studying their morphology, biology, protease activity and the 18S rRNA gene sequence. Morphology of the organism was observed by light microscopy, scanning electron microscopy and transmission electron microscopy. Its structure corresponded to an amphizoic amoeba. The protozoa grew well at 37 °C and poorly at lower temperatures. In addition, it was capable of lysing mammalian cells *in vitro*. A major 56 kDa proteolytic enzyme was observed in amoeba crude extracts by gelatin–sodium dodecyl sulphate–polyacrylamide gel electrophoresis. Most proteolytic enzymes in protozoa extracts showed significant activity over a wide range of pH (3–9) and temperature (8–45 °C) values. The assays on inhibition of protease activity indicated strongly that enzymes detected in amoeba extracts corresponded to serine proteases and, to a lesser extent, cysteine proteases. The use of proteinase inhibitors on a tissue culture model proved that the proteinase activity is critical for developing focal lesions in HeLa cell monolayers. Finally, partial sequencing of the 18S ribosomal RNA gene and phylogenetic analyses indicated that the isolate is closely related to *Acanthamoeba griffini* H37 from the UK (T3 genotype).

Key words: *Acanthamoeba*, pathogenicity, keratitis.

INTRODUCTION

Corneal ulcers are an important worldwide cause of visual morbidity. Epidemiological studies point to facultative parasites, microorganisms or both simultaneously as possible aetiological agents. Among the emerging opportunistic pathogens infecting the human eye, cases of *Acanthamoeba* causing amoebic keratitis are being reported with increasing frequency (Lorenzo-Morales *et al*. 2013), although such prevalent rise may be due in part to the improvement in diagnostic methods, such as confocal microscopy and molecular identification techniques (Heredero-Bermejo *et al*. 2013). *Acanthamoeba* pathogens are ubiquitous, and infection may arise by multiple causes: ocular trauma, contaminated eye lenses, contact with soil and contaminated objects or fluids, including hot or cold tap water (Khan, 2009). In Spain, a number of keratitis cases caused by *Acanthamoeba* sp. have been found (Lorenzo-Morales *et al*. 2011; Arnalich-Montiel *et al*. 2012, 2014). As in other Mediterranean countries, most amoebic isolates from humans belonged to T4 genotype, although occasionally other *Acanthamoeba* genotypes have been diagnosed (Spanakos *et al*. 2006; Ozkoc *et al*. 2008; Yera *et al*. 2008; Gatti *et al*. 2010; Risler *et al*. 2013; Arnalich-Montiel *et al*. 2014). Data concerning molecular epidemiology of *Acanthamoeba* species are relevant since the type of isolate present in a keratitis patient may influence the outcome of the chemotherapy (Heredero-Bermejo *et al*. 2013; Lorenzo-Morales *et al*. 2013). In addition, biochemical characterization of proteases in amoebic isolates has proven to be important to unravel the mechanisms underlying adhesion/penetration and cell lysis in live host tissues (Khan, 2009; Omaña-Molina *et al*. 2013). For all these reasons, the present work was aimed at the characterization of an *Acanthamoeba* isolate obtained from a contact lens wearer in Spain. Results obtained in this work include new and relevant data on ultrastructure, proteases and biology of a pathogenic *Acanthamoeba griffini*. Moreover, this is the first time that a representative of the *Acanthamoeba* T3 genotype has been characterized in Spain.

* Corresponding author: Departamento de Biomedicina y Biotecnología, Grupo ECOMYP, Facultad de Farmacia, Universidad de Alcalá, 28871 Alcalá de Henares, Madrid, Spain. E-mail: angel.criado@uah.es

Parasitology (2015), **142**, 363–373.
doi:10.1017/S0031182014001140

MATERIALS AND METHODS

Isolation and culture of amphizoic amoebae

A female contact lens wearer was examined at the Eye Unit of the Hospital Clínico (Madrid, Spain). Keratitis was diagnosed in only 1 eye and the corresponding contact lens subjected to further examination. The sample was received by the Parasitology Service of the Instituto Carlos III and finally sent to the Parasitology Laboratory (Universidad de Alcalá) for analysis. A sterile cotton swab was rubbed against the inner surface of the patient's contact lens and the sample taken was used for culture tests on non-nutrient agar plates covered with 100 μL of a 24-h-old *Escherichia coli* culture (grown in Mueller-Hinton medium, Scharlau, Barcelona, Spain). In order to bypass axenization of amoebic cultures, bacteria were killed by autoclaving prior to plating on the culture medium. Culture plates were sealed and incubated at 37 °C for 30 days and examined every 48 h for amoebal growth. Positive cultures were diluted to eliminate any coexisting organism and amoebae were transferred to a fresh plate. The environmental isolate *Acanthamoeba castellanii* UAH-T17c3 (isolated from a cooling tower in Madrid, Spain) was used to compare the morphology and proteolytic enzyme activity of the pathogenic and non-pathogenic isolates of *Acanthamoeba* sp. The pathogenic amoeba was grown in 25 cm^2 tissue culture flasks using CERVA liquid medium (Cerva, 1969), which contains 20 g L^{-1} bactocasitone, 10% foetal bovine serum (FBS), 0·1 g L^{-1} streptomycin and 0·06 g L^{-1} penicillin. The environmental isolate was cultured in PYG–bactocasitone liquid medium (0·75%, w/v, proteose peptone; 0·75%, w/v, yeast extract; 2% bactocasitone and 1·5%, w/v, glucose) at 25 °C as described previously by Khan and Paget (2002).

Morphological and ultrastructural studies

Amoebae were subjected to morphological characterization by photonic and confocal microscopy, as well as scanning electron microscopy (SEM) and transmission electron microscopy (TEM). Morphological features were assessed by digital microphotographs obtained with a Motic BA300 microscope using the Motic Images Plus software version 2.0. All measurements were repeated in 15 protozoa and are given as means ± S.D. in micrometres (μm). Exponential phase cultures were used in all trophozoite observations. Death phase cultures (3 weeks old) were employed for recovery of amoebic cysts. For confocal microscopy *Acanthamoeba* trophozoites were stained with 4′,6-diamidino-2-phenylindole (DAPI) and phalloidin–fluorescein isothiocyanate. In short, amoebae aliquots were loaded onto a circular cover glass and incubated at their optimal growth temperature. Immediately after adhesion of protozoa to the slide surface, they were washed 5 times with phosphate buffered saline (PBS). Protozoa were fixed with 3·7% paraformaldehyde in PBS for 15 min at room temperature. Permeabilization of protozoa on coverslips was achieved by subsequent treatment with 0·1% Triton X-100 in PBS for 5 min at room temperature. After 10 washings with PBS, trophozoites were labelled with phalloidin (Invitrogen) for 1 h at 37 °C. Once fluorochrome labelling was completed, the amoebae were washed again 10 times with PBS. Finally, coverslips were mounted using ProLong gold antifade reagent with DAPI (Invitrogen) and incubated at 4 °C overnight. Images were obtained with a Leica TCS-SP5 microscope.

For SEM studies, amoebae were fixed in Milloning's solution containing 2% glutaraldehyde, washed in Milloning's solution with 0·5% glucose and dehydrated first through an ethanol series and finally with anhydrous acetone. Samples were critical-point dried using a Polaron CPD7501 critical-point drying system and sputter coated with 200 Å gold–palladium using a Polaron E5400. SEM was performed at 5–15 kV on a Zeiss DSM 950 SEM. TEM was carried out as follows: amoeba cultures were washed in 0·1 M Milloning's buffer prior to fixation. Protozoa were fixed in 2% glutaraldehyde solution buffered with 0·1 Milloning's buffer at pH 7·2 for 2 h. To facilitate thin section preparation, fixed protozoa were embedded in 2% agar (Dykstra, 1993). Agarized pellets were then fixed in 1% osmium tetroxide, dehydrated in a graded acetone series and embedded in Spurr's resin. Ultramicrotome sections were stained with 1% uranyl acetate followed by 2·5% lead citrate and examined on a Zeiss M10 microscope at 25–30 kV.

Identification and differentiation from other amoeba species were mainly achieved on the basis of: presence of lobopods or filopods, cyst size, number of opercula (also called 'pores' by some authors) and temperature tolerance. The latter was evaluated by growing the pathogenic amoeba at different temperatures (25, 32 and 37 °C) in CERVA liquid medium during 8 days, with cell counts at 48, 96 and 192 h. The inoculum was 6000 amoeba trophozoites mL^{-1} of medium and 5 mL were added into each culture flask.

Pathogenic effects of amoeba trophozoites on mammalian cells

Cytopathic effects caused by the pathogenic amoeba were tested on an immortalized glial cell line isolated from mouse retina (MUPH-1) or alternatively (in protease studies) on human (HeLa) cells. Mammalian cells were routinely cultured in 6-well microplates with commercial Dulbecco's modified Eagle's medium (DMEM) (SIGMA), supplemented with 10% FBS (Lonza Ibérica, Barcelona, Spain) and

https://doi.org/10.1017/S0031182014001140 Published online by Cambridge University Press

1% antimicrobial mix (Lonza Ibérica) containing 100 mg L^{-1} penicillin and 100 mg L^{-1} streptomycin. The cytopathic effect of amoebae was checked visually (by photonic and SEM) and also by an MTT assay where the tetrazolium salt 3-(4,5-dimethylthiazol-2-yl)-2,5-diphenyltetrazolium bromide (SIGMA) was added to the amoeba culture after 6, 12, 18 or 24 h of incubation. Formazan production was quantified in cultures by measuring optical density at 570 nm 4 h after adding MTT (Lagmay *et al*. 1999). In tests aimed at assessing the cytopathic effects caused by amoebae, the standard DMEM (supplemented with FBS) was removed from wells and substituted by fresh DMEM without FBS. After 2 h, amoebic trophozoites were added to mammalian cell cultures. Protozoa were harvested from the axenic cultures by centrifugation (1000 ***g*** for 10 min) and transferred onto a monolayer of MUPH-1 cells at different amoeba:cell ratios ranging from 1:200 to 1:5. In these assays, 1 well was used for the control and 5 wells for testing the pathogenic effect caused by different protozoa inocula ($0{\cdot}2 \times 10^5$, 10^5, $2{\cdot}5 \times 10^5$, 5×10^5 or 10×10^5 trophozoites). At the moment of inoculation with *Acanthamoeba*, each culture well contained an estimate of 5×10^6 mammalian cells. These experiments were run in triplicate. Amoebae were considered highly cytopathic when the monolayer was lysed after 24 h.

Analyses of proteolytic activity in amoeba homogenates and effect of proteinase inhibitors on co-cultures of amoebae and mammalian cell monolayers

Proteases were studied for comparative purposes in both the pathogenic amoeba strain and the environmental isolate *A. castellanii* T17c3. Analyses of proteolytic activity were performed on gelatin–sodium dodecyl sulphate–polyacrylamide gel electrophoresis (SDS–PAGE) gels following the procedure published by Alsam *et al*. (2005). Only amoeba crude extracts were used in these assays. In brief, amoeba cultures were centrifuged at 1000 ***g*** for 10 min at room temperature. Protozoan pellets were resuspended in PBS and disrupted in an ice bath using a MICROSON sonicator (Giltron, Norwood MA, USA). Ultrasounds were applied at 50 W for 50 s, in pulses of 10 s. Protein concentration was measured by the standard Bradford method and adjusted to 1 mg mL^{-1}. Aliquots (50 μL) of the amoeba extract were stored at −20 °C until use. About $1{\cdot}5$ μg of protein were loaded per well for electrophoretic runs. The tolerance of proteases to temperature and pH was tested under the following conditions: pH 3, 5, 7 and 9; temperatures of 8, 25, 37 and 45 °C. The optimum pH value was determined at 37 °C, while the optimum temperature was ascertained at pH 7. Citrate buffer (0·1 M) was employed for proteinase assays run at pH 3 and 5, Tris buffer (0·05 M) for assays at pH 7 and 9. Protease inhibitor assays were performed at 37 °C and pH 7. The following inhibitors were tested: 0·05 mM chymostatin, 50 mM ethylenediaminetetraacetic acid (EDTA), 0·05 mM leupeptin, 5 mM phenylmethylsulfonyl fluoride (PMSF) and 1·5 mM pepstatin A. Amoeba extract aliquots were incubated for 30 min in the presence of inhibitors prior to electrophoresis.

In assays designed to check the effect of protease inhibitors on the pathogenic amoeba isolate and HeLa cell co-cultures, each culture well contained an estimate of 5×10^6 HeLa cells and 3×10^5 amoebic trophozoites. Both control and protease inhibitor-treated amoebae were always included in the assays. Only drugs capable of reducing protease activity *in vitro* (in gelatin–SDS–PAGE analysis) were used in these experiments. Thus, assays included only PMSF (1 mM) or chymostatin (0·05 mM). The test started with the addition of the inhibitor to the amoeba culture medium (see above). After 1 h of incubation with either PMSF or chymostatin, amoebae were recovered by centrifugation, resuspended in culture medium and used to inoculate the human cell culture. The effect of inhibitors on the mammalian/amoeba model system was checked at 12, 24 and 48 h.

All protease-related experiments were repeated at least twice.

Sequencing of the 18S rRNA and phylogenetic analysis

Sequence analysis of the isolate's small ribosomal subunit gene was performed as follows: amoebae were harvested from actively growing axenic cultures by centrifugation at 1000 ***g*** for 10 min. Whole-cell DNA was isolated with the DNAeasy Blood and tissue kit (Qiagen, Hilden, Germany). The 18S rRNA gene was partially amplified using primers CRN5 and 1137 as described by Schroeder *et al*. (2001). Three internal primers (namely 373, 570C and 892C, as published by the aforementioned authors) were used for sequencing purposes. The fragment amplified by primers CRN5 and 1137 is a region of approximately 1500 bp at the 5′ end of the 18S rRNA gene. Polymerase chain reaction (PCR)-amplified products were visualized with ethidium bromide after agarose gel electrophoresis. Bands of interest were excised from gels and purified with the Ultra Clean 15 DNA purification kit (Mobio, Carlsbad, CA, USA). The amplified DNA fragment was sequenced without cloning on an ABI 3130 automated sequencer (Applied Biosystems Inc., Foster City, CA, USA). Three fragments (obtained in different PCR amplifications) were sequenced for the sake of consistency. Sequence data were processed with the BioEdit 5.0.9 sequence editor (Hall, 1999) and then compared against GenBank® databases using a BLASTN search. Clustal Omega (Sievers and Higgins, 2014) was used for pairwise alignments

https://doi.org/10.1017/S0031182014001140 Published online by Cambridge University Press

and phylogenetic analyses were performed with the MEGA 5.0 package software (Tamura *et al*. 2011).

RESULTS

Morphology and ultrastructure

Successful amoebae cultures were prepared from a contact lens provided by the patient. Morphologically, amoeba trophozoites showed acanthopodia, which suggested the presence of *Acanthamoeba, Vahlkampfia* or *Hartmanella* (Fig. 1A and C). Amoebic trophozoites (identified later as *Acanthamoeba* sp. MYP2004, as explained below) were irregular in shape (Fig. 1A). It is important to mention that in trophozoites isolated from the patient (Fig. 1C) the number of acanthopodia observed by SEM was larger than in an environmental *A. castellanii* T17c3 isolate of Spain (Fig. 1D). Likewise, cysts were recovered and observed by photonic microscopy (Fig. 1B) and SEM (Fig. 1E and F). The endocyst was usually star-like, with 6–7 arms (Fig. 1B), unlike the exocyst which showed an irregular spherical shape. When observed by SEM, cysts showed 6 opercula (3–4 of them in each hemisphere; Fig. 1E and F).

Sections of amoebic trophozoites observed under TEM were irregularly ovoid to circular shape. Amoebae emitted numerous fine protoplasmic projections of different lengths on their cell surface (Fig. 2A and B). Large numbers of dark glycogen grains were readily noticed in the cytoplasm (Fig. 2D). There were also noticeable amounts of usually circular-shaped vacuoles of diverse sizes. Excretory vacuoles (Fig. 2B) showed a clear content, whereas the digestive ones (Fig. 2A and D) presented a darker content. Lamellar and residual bodies could be observed in some amoeba sections (Fig. 2D and F). The trophozoite cytoskeleton was minimal and tubulin or actin filaments were not easy to observe. In spite of this finding, confocal microscopy observations with phalloidine staining showed that actin filaments were massively located close to the plasma membrane and inside the acanthopodia (Fig. 2G). Diverse cellular organelles could be observed in amoeba trophozoites. The nucleus was enclosed in a typical nuclear envelope where nuclear pores were difficult to find (Fig. 2F). The single nucleolus was clearly discernable (Fig. 2F). There was also evidence of a quite elaborated Golgi complex, composed of clusters of flattened cisternae (Fig. 2E). In many protozoa, portions of rough Endoplasmic reticulum (ER) were visible, although not especially abundant. Amoebae usually showed a large number of mitochondria dispersed in the cytoplasm (Fig. 2A–C). Some of these observations were confirmed by confocal microscopy and DAPI staining: abundant mitochondria were found dispersed in the protozoan endoplasmic region (Fig. 2H) and chromatin was also evident in the nuclear region of amoebic trophozoites (Fig. 2H).

All these features point to an *Acanthamoeba* sp. isolate as the pathogenic organism causing infection in the contact lens wearer.

Biological features and cytopathogenicity

The isolate *Acanthamoeba* sp. MYP2004 grew poorly in PYG–bactocasitone and therefore the CERVA medium was used in all biological studies related to this strain. In contrast, the environmental isolate *A. castellanii* T17c3 grew better in PYG–bactocasitone (Heredero-Bermejo *et al*. 2012).

Temperature tolerance tests indicated that optimal growth of the pathogenic *Acanthamoeba* sp. MYP2004 isolate was achieved at 37 °C (Fig. 3). On the other hand, amoeba trophozoites produced noticeable cytopathic effects against monolayers of MUPH-1cells (Fig. 1G and H) at these temperatures. The lytic effect was also studied by the MTT assay. The decrease in optical density caused by cell lysis was dependent on the amoebic load introduced in mammalian cell cultures (Fig. 4A). Both microscopy and spectrophotometric monitoring showed that lysis of mammalian cells was partial at 12 h and complete at 24 h when MUPH-1 cell cultures were inoculated with amoeba trophozoites in a ratio of 1:10 or greater. When MUPH-1 cells were incubated with different amounts of amoebae in the presence of MTT, a strong linear relationship between the number of protozoa and the O.D. was found (Fig. 4B, $r = 0{\cdot}96$ at 18 h), which indicates that there is a clear dose–response effect. All these data confirm the presence of a highly pathogenic amoeba in the patient with keratitis.

Analysis of intracellular amoebic proteases and the effect of protease inhibitors on a tissue + amoeba culture model system

Electrophoretic analysis showed that proteases were abundant and highly active in extracts of the pathogenic *Acanthamoeba* sp. MYP2004 isolate. At least 7 different enzymes of molecular weights ranging from 22 to 56 kDa (namely 22, 26, 28, 35, 42, 48 and 56 kDa) were consistently detected in gels (Fig. 5A and B). The 56 kDa protease was highly active. In general, most proteases worked well in a wide range of temperature (25–45 °C) and pH (3–9) values, although 3 of the enzymes (22, 26 and 28 kDa) showed less activity at pH 3 (Fig. 5A and B). All proteases showed lower activity at 8 °C, except for the 56 kDa enzyme (Fig. 5B). When protease inhibitors were tested on amoeba extracts, the protease band at 35 kDa disappeared from the zymograms. Low molecular weight proteases (22, 26 and 28 kDa) were chymostatin-sensitive in inhibition assays, indicating that they belong to the cysteine proteinase family

https://doi.org/10.1017/S0031182014001140 Published online by Cambridge University Press

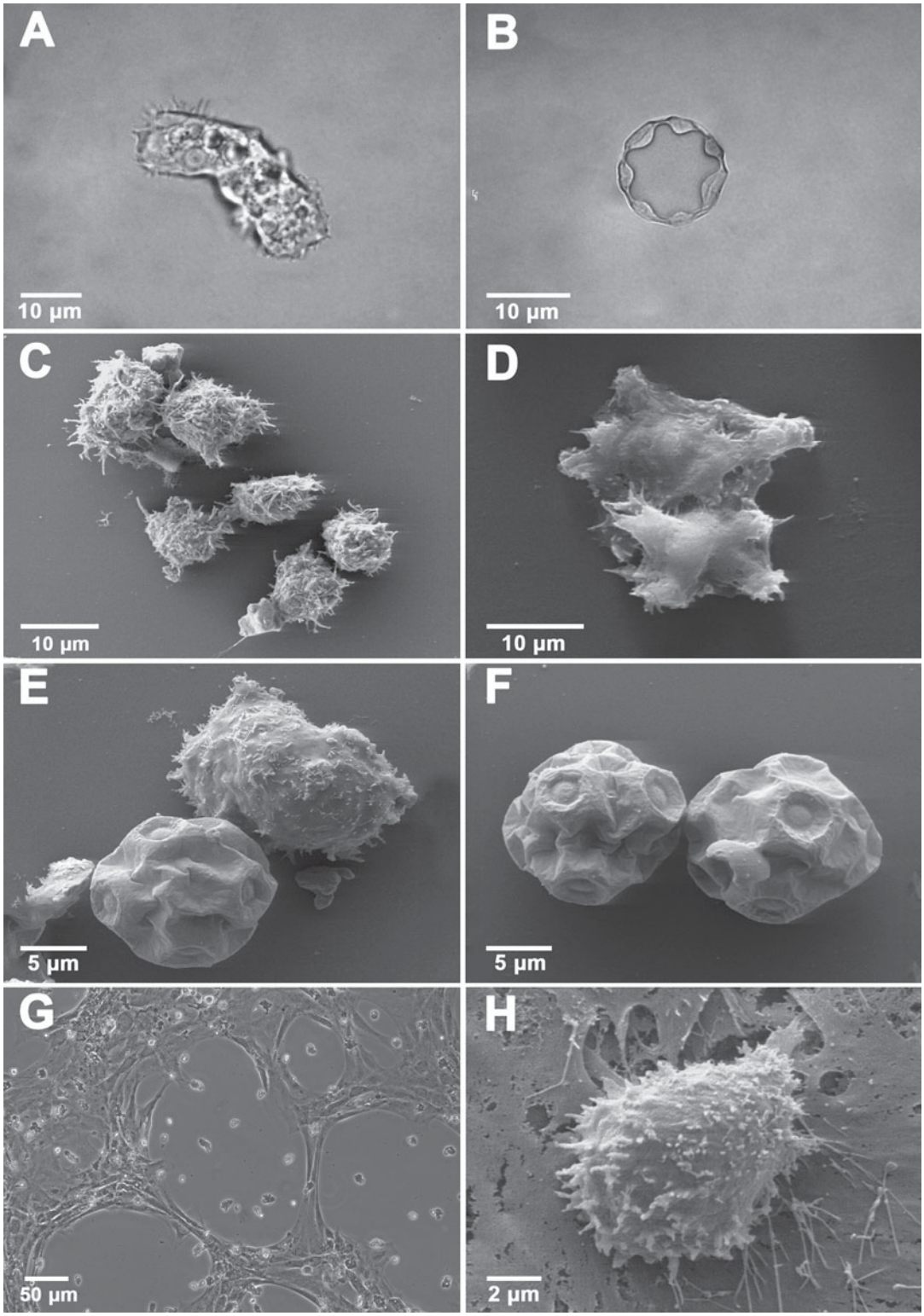

Fig. 1. (A) *Acanthamoeba* sp. (isolate MYP2004) trophozoite as observed by light microscopy; (B) *Acanthamoeba* sp. MYP2004 cyst as seen by photonic microscopy. Note the double-walled structure with a star-like endocyst; (C) *Acanthamoeba* sp. MYP2004 trophozoites as observed by SEM. Note the presence of abundant acanthopodia with evident adherence to the substrate; (D) *A. castellanii* T17c3 trophozoites as observed by SEM. The presence of acanthopodia is less frequent in this environmental isolate than in the pathogenic *Acanthamoeba* sp. MYP2004; (E) *Acanthamoeba* sp. MYP2004 trophozoite and cyst as observed by SEM; (F) *Acanthamoeba* sp. MYP2004 cysts as seen by SEM. The exocyst is roughly spherical, with its surface notably wrinkled. Usually, 3 opercula (pores) may be readily observed in the visible cyst hemisphere; (G) immortalized glial mouse retina cells as seen by photonic microscopy after 18 h of incubation at 37 °C with *Acanthamoeba* sp. MYP2004 trophozoites (initial inoculum of 10^5 amoebae); (H) SEM image of an amoebic trophozoite (after the same incubation period as in (G). Note how the protozoan acanthopodia adhere to mammalian cells, with evidence of membrane disruption of the target cell at the contact site.

https://doi.org/10.1017/S0031182014001140 Published online by Cambridge University Press

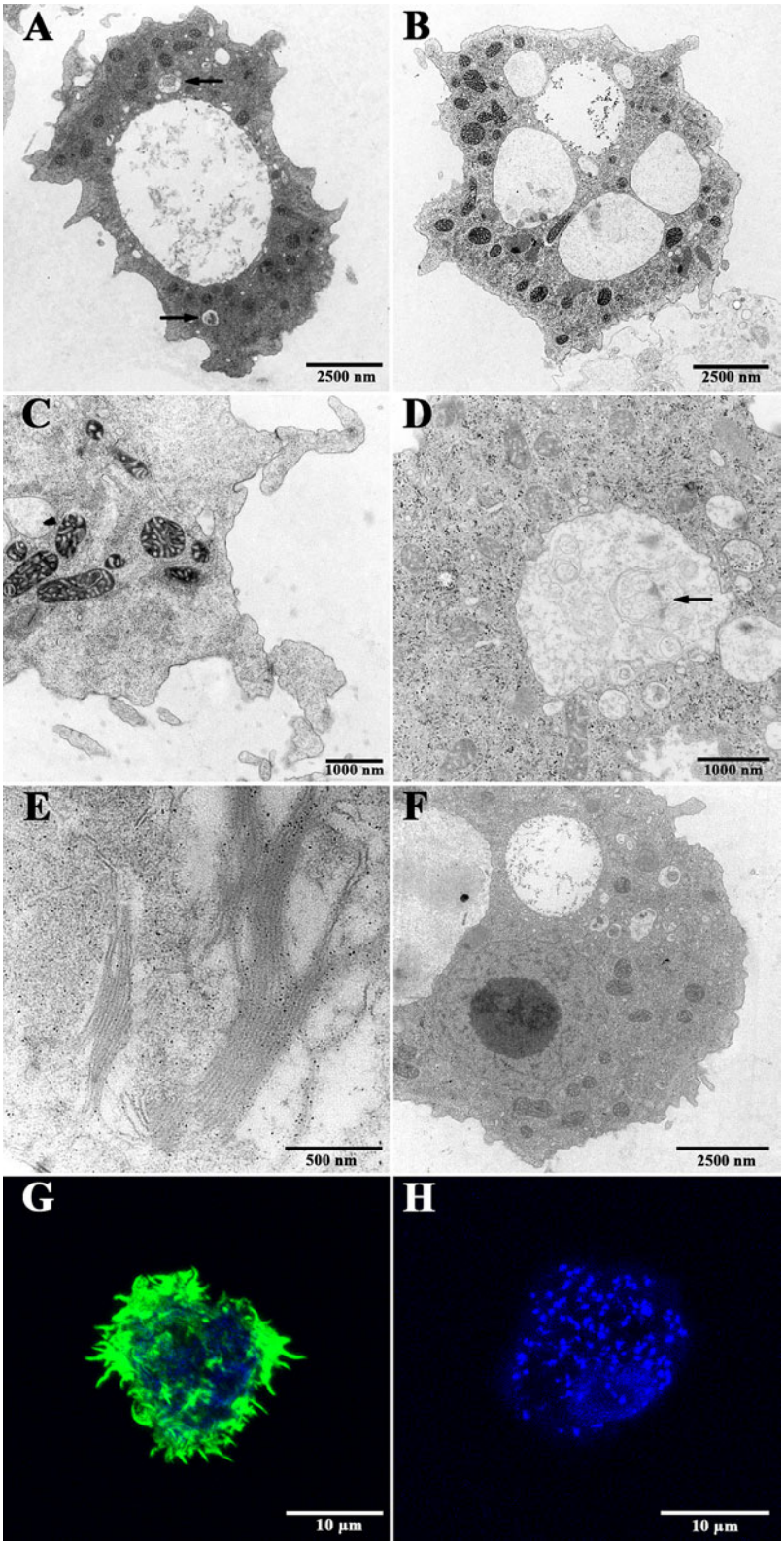

Fig. 2. Ultrastructure of *Acanthamoeba* sp. MYP2004 as observed by TEM, and detection of some intracellular components in trophozoites by confocal microscopy. (A) Thin section of an *Acanthamoeba* sp. MYP2004 trophozoite observed by TEM showing an oval-shaped cellular body section, some acanthopodia on the cell surface, a large excretory vacuole, some digestive vacuoles (arrows) and numerous mitochondria; (B) *Acanthamoeba* sp. MYP2004 trophozoite showing several vacuoles with an either clear or electrodense content. Numerous mitochondria are also evident; (C) TEM details of an *Acanthamoeba* sp. MYP2004 trophozoite containing abundant mitochondria with tubular cristae; (D) amoeba trophozoite thin section as observed by TEM. The cytoplasm is a granular matrix containing dark granules (possibly glycogen). Lamellar bodies may be also observed in the central vacuole (arrow); (E) Golgi apparatus in an *Acanthamoeba* sp. MYP2004 trophozoite. Cisternae are stacked upon each other in up to

https://doi.org/10.1017/S0031182014001140 Published online by Cambridge University Press

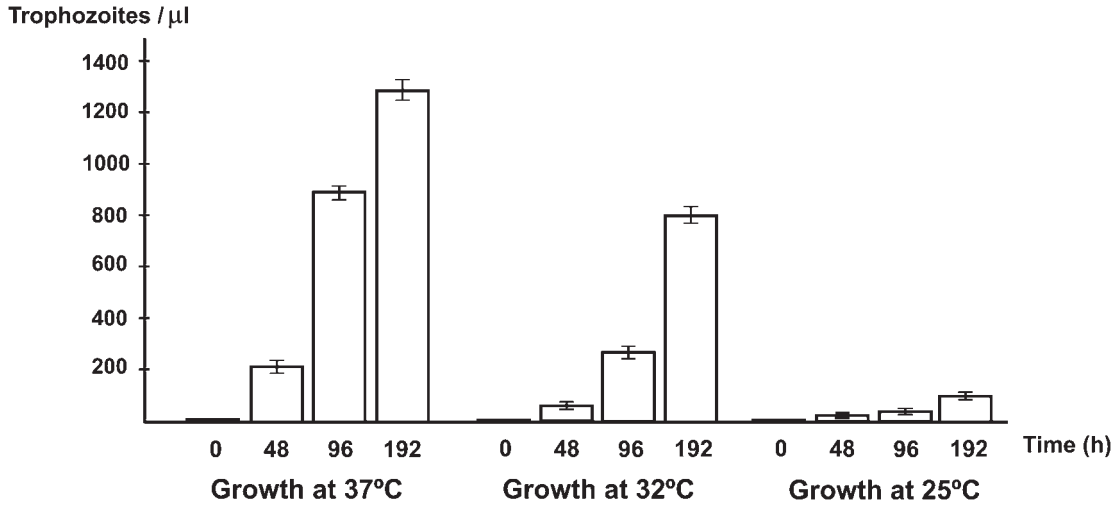

Fig. 3. Growth rates obtained for the pathogenic *Acanthamoeba* sp. MYP2004 isolate grown for 0, 48, 96 and 192 h at different temperatures (37, 32 and 25 °C).

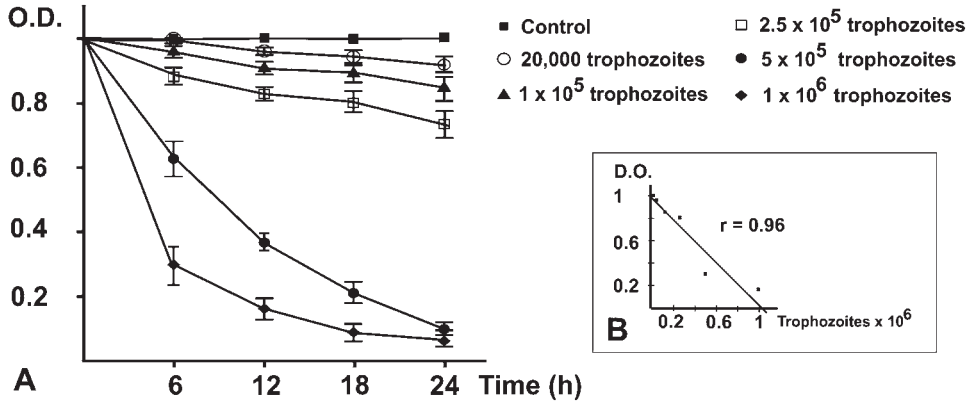

Fig. 4. *Acanthamoeba*-induced lysis of cultured MUPH-1 mouse retina cells. (A) MTT degradation at different times of incubation. Amoeba trophozoites (*Acanthamoeba* sp. MYP2004) were added at 5 different rates and MTT levels monitored in triplicate at 6, 12, 18 and 24 h of incubation. A value of O.D. = 1 was assigned to the cell density in the control well. Lysis of mouse retina cell monolayers occurred at 24 h or earlier for the 2 larger inocula; (B) (inset) regression analysis of O.D. *vs* initial amoeba counts at 18 h of incubation. There is a clear dose–response effect, as judged by the high correlation coefficient ($r = 0{\cdot}96$).

(Fig. 5C). In addition, all proteolytic enzymes were PMSF-sensitive which proves that they are serine proteinases (Fig. 5C).

The environmental isolate *A. castellanii* T17c3 showed consistent protease activity at molecular weights of 24, 30, 32, 45, 49 and 59 kDa (Fig. 5A and B). Interestingly, *A. castellanii* T17c3 proteinases seemed to be less active than those of *Acanthamoeba* sp. MYP2004, since equivalent amounts of protein were loaded on the gels. The 59 kDa proteinase was the most active in *A. castellanii* T17c3 (Fig. 5A and B). Several weak protease bands at 40, 62 and 64 kDa were only active at pH 3 (Fig. 5A), all the rest of proteases showing significant activity at pH 5–9 and temperatures between 25 and 37 °C (Fig. 5A and B). The 24 and 30 kDa bands were not observed when proteinase inhibitors were tested (Fig. 5C). All proteolytic enzymes in *A. castellanii* T17c3 were PMSF-sensitive (Fig. 5C). In addition, the 32 kDa protease was as well chymostatin-sensitive (Fig. 5C) and also less active at pH 3 (Fig. 5A).

When *Acanthamoeba* sp. MYP2004 trophozoites were incubated in the presence of chymostatin, subsequent inoculation of HeLa cell monolayer cultures

3–7 layers; (F) details of the nucleus (Ø 4·8 µM) and the single nucleolus (Ø 2·5 µM) of *Acanthamoeba* sp. MYP2004; (G) confocal microscopy image of a phalloidin-stained *Acanthamoeba* sp. MYP2004 trophozoite. Actin seems to be primarily linked to acanthopodia, close to the cell surface; (H) confocal microscopy image of a DAPI-stained *Acanthamoeba* sp. MYP2004 trophozoite. All mitochondria dispersed in the amoeba cytoplasm and the nucleus (bottom right side) show a strong fluorescent signal.

https://doi.org/10.1017/S0031182014001140 Published online by Cambridge University Press

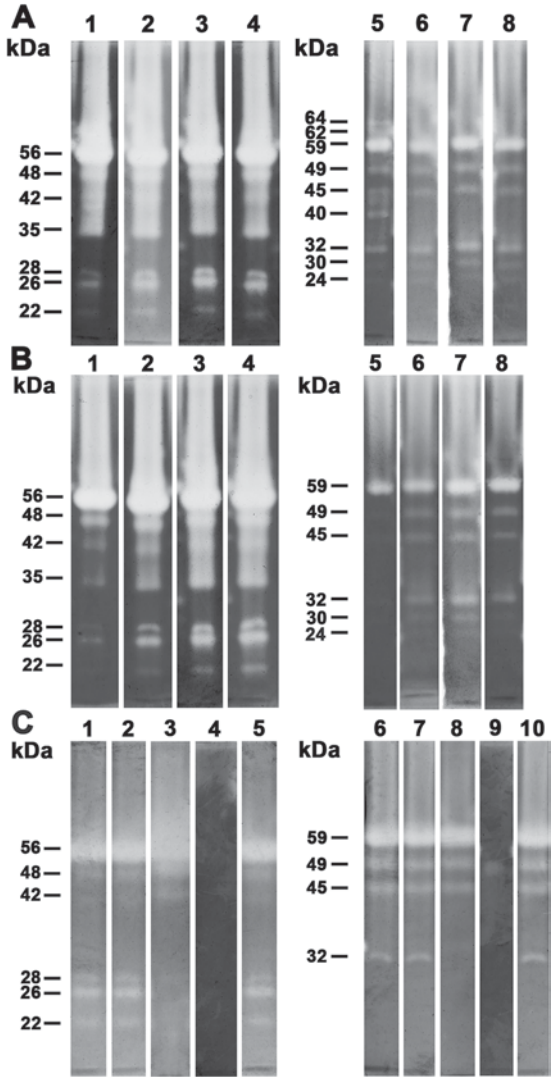

Fig. 5. Comparative analysis of the effect of pH (A), temperature (B) and inhibitors (C) on the proteolytic activity in crude extracts of the pathogenic *Acanthamoeba* sp. MYP2004 and *A. castellanii* T17c3 on protease zymograms in 7·5% gelatin–polyacrylamide gels. Approximate molecular weights of protease bands are indicated on the left. (A) pH 3, 5, 7 and 9 (37 °C), lanes 1–4 (*Acanthamoeba* sp. MYP2004) and lanes 5–8 (*A. castellanii* T17c3), respectively; (B) 8, 25, 37 and 45 °C (pH 7), lanes 1–4 (*Acanthamoeba* sp. MYP2004) and lanes 5–8 (*A. castellanii* T17c3), respectively; (C) inhibitors: EDTA, leupeptin, chymostatin, PMSF and pepstatin A, lanes 1–5 (*Acanthamoeba* sp. MYP2004) and lanes 6–10 (*A. castellanii* T17c3), respectively.

with treated amoebae caused no focal lesions throughout the complete period of observation (12–48 h) (data not shown). In contrast, when amoebae were treated with PMSF, focal lesions appeared at 12 h, the same as in the controls.

Sequencing of the 18S rRNA gene and phylogenetic analyses

The partial 18S rRNA gene sequence obtained in the pathogenic *Acanthamoeba* sp. MYP2004 isolate from Spain showed more than 99% sequence identity to *A. griffini* from the UK (GenBank® accession number S81337) when running a BLAST search. Phylogenetic analyses showed that the Spanish protozoa grouped with other *A. griffini* and *Acanthamoeba pearcei* isolates from the UK and the USA (Fig. 6). The T3 genotype node showed relatively high bootstrap values suggesting real biological significance. Therefore, taking into account both morphological and genetic data the amoebic isolate from Spain was identified in GenBank® as *A. griffini*, registered under accession number KF010846 (isolate MYP2004).

DISCUSSION

Over the last 40 years it has become apparent that some amphizoic amoeba, such as *Acanthamoeba*, *Vahlkampfia* or *Hartmannella* can be associated with keratitis (Walochnik *et al*. 2000). Diverse *Acanthamoeba* species have been reported to cause keratitis, including representatives of genotypes T4, T6 and T11 and to a lesser extent of genotypes T1, T3, T7, T10 and T14 (Maubon *et al*. 2012). Nevertheless, the pathogenic isolate characterized in the present study has been identified as *A. griffini*, a member of the T3 genotype. The Spanish *A. griffini* MYP2004 showed the typical features of pathogenic *Acanthamoeba* isolates: optimal growth when cultured at 37 °C, large number of filopods, high level of proteolytic activity and the ability to cause lysis of cultured mammalian cells (Khan, 2009).

Amoebic isolates can easily be recognized as belonging to the genus *Acanthamoeba* for their polygonal cysts. However, accurate species determination by morphology is still problematic. In our case, both trophozoite and cyst morphologies were similar to those previously described for *A. griffini* in the UK by Ledee *et al*. (1996). Nevertheless, it is important to underline that these authors only observed the amoeba under photonic microscopy. In general, the ultrastructure of *A. griffini* trophozoites and cysts is similar to that of other *Acanthamoeba* sp. (González-Robles *et al*. 2013). The cystic stage morphology as a paramount issue in protozoa taxonomy has been pointed out previously (Janovy *et al*. 2007). However, caution must be exercised in considering only morphological criteria for species determination, and may be confusing due to the pleomorphism of the cultured protozoa (Ledee *et al*. 1996). In agreement with previous studies, genetic analysis has been decisive in the identification of amphizoic amoeba isolates (Stothard *et al*. 1998). It is worth mentioning that members of the *Acanthamoeba* genus are polymorphic in their 18S rRNA sequences, which somewhat complicates the task of molecular identification. Unfortunately, most ribosomal sequences obtained in clinical isolates of *Acanthamoeba* are short often leading only to identification at genotypic clade level. In this sense, reading sufficient sequence information

https://doi.org/10.1017/S0031182014001140 Published online by Cambridge University Press

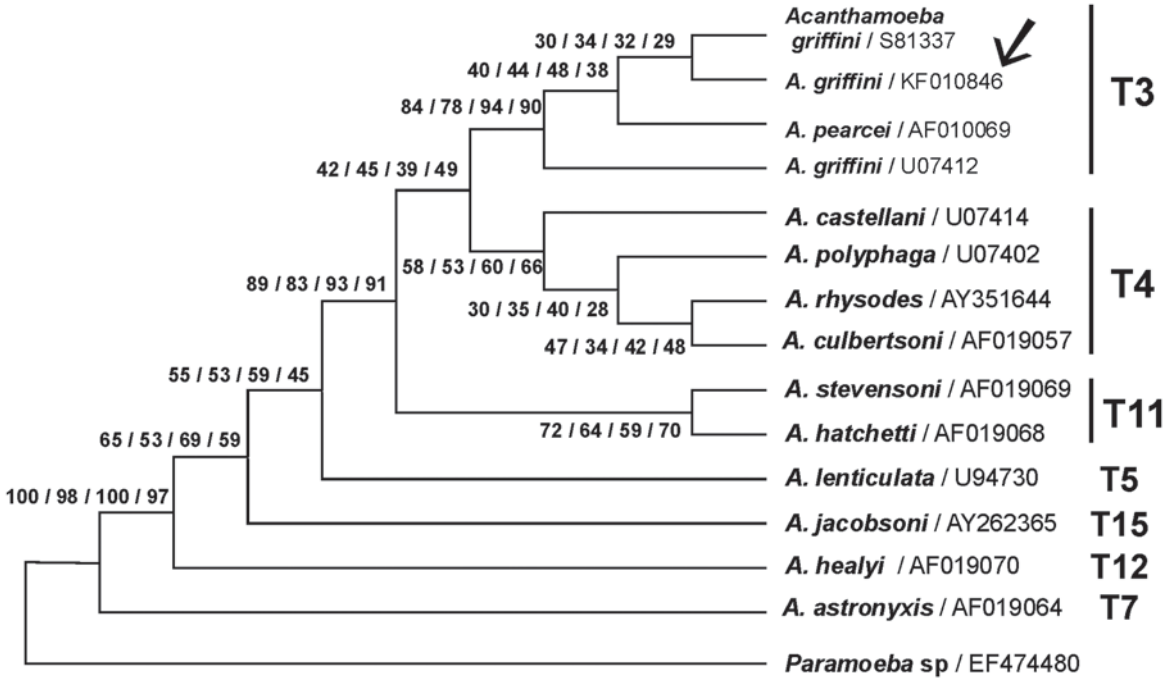

Fig. 6. Phylogenetic relationship of *Paramoeba* sp. (as outgroup) and diverse *Acanthamoeba* species based on the DNA sequence variation of the 18S rRNA gene (MEGA 5 program). GenBank® accession numbers are indicated after each name. The tree was inferred by using the maximum parsimony model. Numbers at nodes indicate boostrap support with 100 replications for 4 different phylogenetic analysis methods: parsimony, maximum composite likelihood with neighbour joining (with Kimura 2-parameter model or Tamura 3-parameter model) and finally UPGMA with Tamura 3-parameter model. The new *A. griffini* sequence (isolate MYP2004, GenBank® accession number KF010846) is indicated by an arrow.

is advisable, which ought to include the 5′ end of the small ribosomal subunit gene. This region is ideal for DNA barcoding in many organisms (Criado-Fornelio, 2012). Such an approach, along with the use of phylogenetic procedures, yields more accurate identifications, as demonstrated for the Spanish *A. griffini* isolate reported in this paper. A search in the GenBank® Nucleotide database for sequences of pathogenic *Acanthamoeba* in Spain led to just 2 isolates, 1 member of the T4 genotype (*Acanthamoeba* sp., reported by Arnalich-Montiel *et al*. 2012) and another of the T11 genotype (*Acanthamoeba polyphaga*, reported by Lorenzo-Morales *et al*. 2011). Similar findings have been published in Italy, where only *Acanthamoeba* T4 representatives were found as keratitis-causing organisms in 10 patients (Gatti *et al*. 2010). Reports on pathogenic T3 isolates in Europe are scarce; they have been found in the UK (Ledee *et al*. 1996) and Central France (Risler *et al*. 2013) and recently in Spain (Arnalich-Montiel *et al*. 2014). Some other studies in France failed to detect this genotype (T3) in humans (Yera *et al*. 2008; Maubon *et al*. 2012). The same is true for Greece (Spanakos *et al*. 2006), Turkey (Ozkoc *et al*. 2008) and Austria (Walochnik *et al*. 2000).

Acanthamoeba griffini MYP2004 proteases showed higher enzymatic activity than those of *A. castellanii* T17c3 under different pH and temperature conditions. A similar profile has also been observed in other pathogenic *Acanthamoeba* isolates (Khan, 2009). The comparison of findings on proteases detected in different *Acanthamoeba* sp. is complicated by the low accuracy in determining the proteins' molecular weight in polyacrylamide gels (Serrano-Luna *et al*. 2006). On the other hand, it is worth mentioning that when proteinase inhibitors were tested in the present work, some enzymes could not be detected on zymograms. The explanation for this may rely on the fact that amoeba crude extracts were incubated with inhibitors for 30 min prior to electrophoresis. Hence, some proteinases released by sonication from subcellular compartments might have degraded other cleavage-sensitive proteases present in the samples during incubation.

Most studies on *Acanthamoeba* proteolytic enzymes indicate that serine proteases are very common among members of this genus (Omaña-Molina *et al*. 2013), although cysteine (Leitsch *et al*. 2010) and metalloproteases (Alsam *et al*. 2005) have been reported as well. In the present study both serine and cysteine proteases have been found for the first time in *A. griffini* MYP2004. It is interesting to underline that 3 low molecular weight proteases were inhibited by both PMSF and chymostatin. Such dual-natured proteases have been reported in other *Acanthamoeba* species, such as *A. castellanii* (Na *et al*. 2001). Cysteine proteinases are mainly lysosomal enzymes, employed for intracellular digestion

https://doi.org/10.1017/S0031182014001140 Published online by Cambridge University Press

(Sajid and McKerrow, 2002). Since lysis of HeLa cells caused by *A. griffini* MYP2004 was not observed in the presence of chymostatin, the hypothesis that this inhibitor merely arrested lysosomal activity inside the amoeba cannot be disregarded. If the cellular machinery for digestion is stopped, amoebae would be paralyzed and liberation of other proteases and phagocytosis of mammalian cells impaired. A previous report by Serrano-Luna *et al*. (2006) showed that a pathogenic *A. castellanii* isolate contained 2 proteases of 30 and 34 kDa, which might be the same proteases reported in *A. castellanii* T17c3 in the present work. Nevertheless, the aforementioned authors did not test chymostatin as protease inhibitor and therefore it was concluded that only serine proteinases were present in this species. On the other hand, it is difficult to find an explanation for the fact that, unlike chymostatin, PMSF did not inhibit cell lysis in co-cultures of amoebae and HeLa cells. Other authors (Serrano-Luna *et al*. 2006) reported opposite results, since they failed to observe focal lesions in co-cultures where either *A. polyphaga* or *A. castellanii* had been previously treated with PMSF. Further research into the roles played by proteases in cellular pathogenicity of *A. griffini* is needed. One promising area is siRNA which has been shown to cause a reduction in both serine protease activity and amoebic cytotoxicity in other *Acanthamoeba* species (Lorenzo-Morales *et al*. 2005, 2010).

The treatment of *Acanthamoeba* keratitis is long, troublesome and its outcome highly variable depending on the protozoa species or isolate infecting the patient's eye (Lorenzo-Morales *et al*. 2013). Therefore, a better understanding of the molecular epidemiology of *Acanthamoeba* sp. should be considered a priority (Khan, 2009), as it may well provide clues for effective chemotherapy protocols in different geographic areas.

ACKNOWLEDGEMENTS

We wish to thank Isabel Trabado and Cristina de Miguel (Cell Culture Unit – CAI Medicina y Biología de la Universidad de Alcalá) for technical assistance, Antonio Priego and Mr José Antonio Pérez (Microscopy Unit – CAI Medicina y Biología de la Universidad de Alcalá) for assistance with scanning electron microscopy, Dr Javier Martinez for his valuable help and suggestions, Dr Pedro de la Villa (Department of System's Biology, Universidad de Alcalá) for kindly providing the mammalian cell line and Ángel Pueblas (Photography Unit – CAI Medicina y Biología de la Universidad de Alcalá) for expert help with photographic work.

FINANCIAL SUPPORT

This work was supported by the grants provided by a fellowship from the Ministerio de Educación y Ciencia (FPU ref. AP2010-1471), and the Consejería de Educación de la Comunidad de Madrid and Fondo Social Europeo (F.S.E.) for S.G.G. Fondos de Investigación Sanitaria (FIS) (PI080222), CTQ2011-23245 (MEyC), Consorcio NANODENDMED ref S2011/BMD-2351 (CAM) and CIBER-BBN to U.A. CIBER-BBN is an initiative funded by the VI National R&D&i Plan 2008–2011, Iniciativa Ingenio 2010, Programa de Consolidación, acciones CIBER and financed by the Instituto de Salud Carlos III with assistance from the European Regional Development Fund.

REFERENCES

Alsam, S. A., Sissons, J., Jayasekera, S. and Khan, N. A. (2005). Extracellular proteases of *Acanthamoeba castellanii* (encephalitis isolate belonging to T1 genotype) contributed to increased permeability in an *in vitro* model of the human blood–brain barrier. *The Journal of Infection* **51**, 150–156. doi: 10.1016/j.jinf.2004.09.001.

Arnalich-Montiel, F., Almendral, A., Arnalich, F., Valladares, B. and Lorenzo-Morales, J. (2012). Mixed *Acanthamoeba* and multidrug-resistant *Achromobacter xyloxidans* in late-onset keratitis after laser *in situ* keratomileusis. *Journal of Cataract and Refractive Surgery* **38**, 1853–1856. doi: 10.1016/j.jcrs.2012.08.022.

Arnalich-Montiel, F., Lumbreras-Fernández, B., Martín-Navarro, C. M., Valladares, B., Lopez-Velez, R., Morcillo-Laiz, R. and Lorenzo-Morales, J. (2014). Influence of *Acanthamoeba* genotype on clinical course and outcomes for patients with *Acanthamoeba* keratitis in Spain. *Journal of Clinical Microbiology* **52**, 1213–1216. doi: 10.1128/JCM.00031-14.

Cerva, L. (1969). Amoebic meningoencephalitis: axenic culture of *Naegleria*. *Science* **163**, 576.

Criado-Fornelio, A. (2012). Chapter 1. Emerging protozoal tick-borne diseases of canids (piroplasmosis and hepatozoonosis): impact on wildlife conservation. In *Carnivores: Species, Conservation and Management* (ed. Álvares, F. I. and Mata, G. E.), pp. 1–48. Nova Science Publishers, Hauppage, New York, USA.

Dykstra, M. J. (1993). Agar embedment of cell suspensions or subcellular particulates for transmission electron microscopy. In *A Manual of Applied Techniques for Biological Electron Microscopy* (ed. Dykstra, D. J.), pp. 107–108. Plenum Press, New York, USA.

Gatti, S., Rama, P., Matuska, S., Berrilli, F., Cavallero, A., Carletti, S., Bruno, A., Maserati, R. and Di Cave, D. (2010). Isolation and genotyping of *Acanthamoeba* strains from corneal infections in Italy. *Journal of Medical Microbiology* **59**, 1324–1330. doi: 10.1099/jmm.0.019786-0.

González-Robles, A., Salazar-Villatoro, L., Omaña-Molina, M., Lorenzo-Morales, J. and Martínez-Palomo, A. (2013). *Acanthamoeba royreba*: morphological features and *in vitro* cytopathic effect. *Experimental Parasitology* **133**, 369–375. doi: 10.1016/j.exppara.2013.01.011.

Hall, T. A. (1999). BioEdit: a user-friendly biological sequence alignment editor and analysis program for Windows 95/98/NT. *Nucleid Acids Symposium Series* **41**, 95–98.

Heredero-Bermejo, I., San Juan Martin, C., Soliveri de Carranza, J., Copa-Patiño, J. L. and Pérez-Serrano, J. (2012). *Acanthamoeba castellanii: in vitro* UAH-T17c3 trophozoite growth study in different culture media. *Parasitology Research* **110**, 2563–2567. doi: 10.1007/s00436-011-2761-1.

Heredero-Bermejo, I., Copa-Patiño, J. L., Soliveri, J., García-Gallego, S., Rasines, B., Gómez, R., de la Mata, F. J. and Pérez-Serrano, J. (2013). *In vitro* evaluation of the effectiveness of new water-stable cationic carbosilane dendrimers against *Acanthamoeba castellanii* UAH-T17c3 trophozoites. *Parasitology Research* **112**, 961–969. doi: 10.1007/s00436-012-3216-z.

Janovy, J., Jr. Detwiler, J., Schwank, S., Bolek, M. G., Knipes, A. K. and Langford, G. J. (2007). New and emended descriptions of gregarines from flour beetles (*Tribolium* spp. and *Palorus subdepressus*: Coleoptera, Tenebrionidae). *The Journal of Parasitology* **93**, 1155–1170. doi: 10.1645/GE-1090R.1.

Khan, N. A. (2009). *Acanthamoeba: Biology and Pathogenesis*, pp. 1–209. Caister Academic Press, Norfolk, UK.

Khan, N. A. and Paget, T. A. (2002). Molecular tools for speciation and epidemiological studies of *Acanthamoeba*. *Current Microbiology* **44**, 444–449.

Lagmay, J. P., Matias, R. R., Natividad, F. F. and Enriquez, G. L. (1999). Cytopathogenicity of *Acanthamoeba* isolates on rat glial C6 cell line. *The Southeast Asian Journal of Tropical Medicine and Public Health* **30**, 670–677.

Ledee, D. L., Hay, J., Thomas, F., Byers, T. J., Seal, D. V. and Kirknessf, C. M. (1996). *Acanthamoeba griffini*: molecular characterisation

of a new corneal pathogen. *Investigative Ophthalmology and Visual Science* **37**, 544–550.

Leitsch, D., Köhsler, M., Marchetti-Deschmann, M., Deutsch, A., Allmaier, G., Duchêne, M. and Walochnik, J. (2010). Major role for cysteine proteases during the early phase of *Acanthamoeba castellanii* encystment. *Eukaryotic Cell* **9**, 611–618. doi: 10.1128/EC.00300-09.

Lorenzo-Morales, J., Ortega-Rivas, A., Foronda, P., Abreu-Acosta, N., Ballart, D., Martínez, E. and Valladares, B. (2005). RNA interference (RNAi) for the silencing of extracellular serine proteases genes in *Acanthamoeba*: molecular analysis and effect on pathogenicity. *Molecular and Biochemical Parasitology* **144**, 10–15. doi: 10.1128/AAC.00329-10.

Lorenzo-Morales, J., Martín-Navarro, C. M., López-Arencibia, A., Santana-Morales, M. A., Afonso-Lehmann, R. N., Maciver, S. K., Valladares, B. and Martínez-Carretero, E. (2010). Therapeutic potential of a combination of two gene-specific small interfering RNAs against clinical strains of *Acanthamoeba*. *Antimicrobial Agents and Chemotherapy* **54**, 5151–5155. doi: 10.1128/AAC.00329-10.

Lorenzo-Morales, J., Morcillo-Laiz, R., Martín-Navarro, C. M., López-Vélez, R., López-Arencibia, A., Arnalich-Montiel, F., Maciver, S. K., Valladares, B. and Martínez-Carretero, E. (2011). *Acanthamoeba* keratitis due to genotype T11 in a rigid gas permeable contact lens wearer in Spain. *Contact Lens and Anterior Eye: The Journal of the British Contact Lens Association* **34**, 83–86. doi: 10.1016/j.clae.2010.10.007.

Lorenzo-Morales, J., Martín-Navarro, C. M., López-Arencibia, A., Arnalich-Montiel, F., Piñero, J. E. and Valladares, B. (2013). *Acanthamoeba* keratitis: an emerging disease gathering importance worldwide? *Trends in Parasitology* **29**, 181–187. doi: 10.1016/j.pt.2013.01.006.

Maubon, D., Dubosson, M., Chiquet, C., Year, H., Brenier-Pinchart, M. P., Cornet, M., Savy, O., Renard, E. and Pelloux, H. (2012). A one-step multiplex PCR for *Acanthamoeba* keratitis diagnosis and quality samples control. *Investigative Ophthalmology and Visual Science* **53**, 2866–2872. doi: 10.1167/iovs.11-8587.

Na, B. K., Kim, J. C. and Song, C. Y. (2010). Characterization and pathogenetic role of proteinase from *Acanthamoeba castellanii*. *Microbial Pathogenesis* **30**, 39–48. doi: 10.1006/mpat.2000.0403.

Omaña-Molina, M., González-Robles, A., Salazar-Villatoro, L. I., Lorenzo-Morales, J., Cristóbal-Ramos, A. R., Hernández-Ramírez, V. I., Talamás-Rohana, P., Méndez- Cruz, A. R. and Martínez-Palomo, A. (2013). Reevaluating the role of *Acanthamoeba* proteases in tissue invasion: observation of cytopathogenic mechanisms on MDCK cell monolayers and hamster corneal cells. *BioMed Research International* **2013**, 461329. doi: 10.1155/2013/461329.

Ozkoc, S., Tuncay, S., Delibas, S. B., Akisu, C., Ozbek, Z., Durak, I. and Walochnik, J. (2008). Identification of *Acanthamoeba* genotype T4 and *Paravahlkampfia* sp. from two clinical samples. *Journal of Medical Microbiology* **57**, 392–396. doi: 10.1099/jmm.0.47650-0.

Risler, A., Coupat-Goutaland, B. and Pélandakis, M. (2013). Genotyping and phylogenetic analysis of *Acanthamoeba* isolates associated with keratitis. *Parasitology Research* **112**, 3807–3816. doi: 10.1007/s00436-013-3572-3.

Sajid, M. and McKerrow, J. H. (2002). Cysteine proteases of parasitic organisms. *Molecular and Biochemical Parasitology* **120**, 1–21. doi: 10.1016/S0166-6851(01)00438-8.

Schroeder, J. M., Booton, G., Hay, J., Niszl, I. A., Seal, D. V., Markis, M. B., Fuerst, P. A. and Byers, T. J. (2001). Use of subgenic 18S ribosomal DNA PCR and sequencing for genus and genotype identification of *Acanthamoeba* from humans with keratitis and from sewage sludge. *Journal of Clinical Microbiology* **39**, 1903–1911. doi: 10.1128/JCM.39.5.1903-1911.2001.

Serrano-Luna, J. J., Cervantes, I., Calderon, J., Navarro, F., Tsutsumi, V. and Shibayama, M. (2006). Protease activities of *Acanthamoeba polyphaga* and *A. castellanii*. *Canadian Journal of Microbiology* **52**, 16–23. doi: 10.1139/w05-114.

Sievers, F., Higgins, D. G. (2014). Clustal Omega, accurate alignment of very large numbers of sequences. *Methods in Molecular Biology* **1079**, 105–116. doi: 10.1007/978-1-62703-646-7_6.

Spanakos, G., Tzanetou, K., Miltsakakis, D., Patsoula, E., Malamou-Lada, E. and Vakalis, N. C. (2006). Genotyping of pathogenic *Acanthamoebae* isolated from clinical samples in Greece – report of a clinical isolate presenting T5 genotype. *Parasitology International* **55**, 147–149. doi: 10.1016/j.parint.2005.12.001.

Stothard, D. R., Schroeder-Diedrich, J. M., Awwad, M. H., Gast, R. J., Leder, D. R., Rodríguez-Zaragoza, S., Dean, C. L., Fuerts, D. A. and Byers, T. J. (1998). The evolutionary history of the genus *Acanthamoeba* and the identification of eight new 18S rRNA gene sequences. *Journal of Eukaryotic Microbiology* **45**, 45–54.

Tamura, S., Peterson, D., Peterson, N., Stecher, G., Nei, M. and Kumar, S. (2011). MEGA5: molecular evolutionary genetics analysis using maximum likelihood, evolutionary distance and maximum parsimony methods. *Molecular Biology and Evolution* **28**, 2731–2739. doi: 10.1093/molbev/msr121.

Walochnik, J., Haller-Schober, E., Kölli, H., Picher, O., Obwaller, A. and Aspöck, H. (2000). Discrimination between clinically relevant and nonrelevant *Acanthamoeba* strains isolated from contact lens-wearing keratitis patients in Austria. *Journal of Clinical Microbiology* **38**, 3932–3936.

Yera, H., Zamfir, O., Bourcier, T., Viscogliosi, E., Noël, C., Dupouy-Camet, J. and Chaumeil, C. (2008). The genotypic characterisation of *Acanthamoeba* isolates from human ocular samples. *British Journal of Ophthalmology* **92**, 1139–1141. doi: 10.1136/bjo.2007.132266.